

# Seismic and Tsunamis Vulnerability Assessment of the Shelter School Building Structure with and without Retrofitting

Fauzan<sup>1\*</sup>, Zev Al Jauhari<sup>2</sup>, Geby Aryo Agista<sup>1</sup>, Atsushi Yokota<sup>3</sup>, Masharya Eko Putra<sup>1</sup>

<sup>1</sup>Department of Civil Engineering, Andalas University, Padang, INDONESIA

<sup>2</sup>Graduate School of Engineering, Toyohashi University of Technology, Toyohashi, JAPAN

<sup>3</sup>Department of Architecture and Civil Engineering, Toyohashi University of Technology, Toyohashi, JAPAN

\*Corresponding author: [fauzan@eng.unand.ac.id](mailto:fauzan@eng.unand.ac.id)

SUBMITTED 21 May 2024 REVISED 06 September 2024 ACCEPTED 11 October 2024

**ABSTRACT** Understanding the vulnerability of school shelters to tsunamis is crucial for developing effective mitigation strategies and increasing the resilience of coastal communities in the education sector. SDN 02 Sasak Ranah Pasisia, an elementary school in West Pasaman Regency, West Sumatera, Indonesia, had a shelter building constructed in 2010. However, the construction remains incomplete. A structural assessment using current Indonesian building codes and vulnerability analysis is necessary to proceed with construction and ensure the building's strength against the working loads. The structural assessment revealed that several columns could not support the working load, necessitating local retrofitting. In this study, the retrofitting of the building was designed using concrete jacketing. Furthermore, structural fragility curves of the school building were developed before and after retrofitting against earthquake and tsunami loads. The seismic fragility curve was determined from the maximum displacement of the building for varied earthquake acceleration, using nonlinear time history dynamic response analysis scaled using the incremental dynamic analysis method and damage limits defined by ATC-40, characterized by Hazus. Meanwhile, the tsunami fragility curve was determined from the maximum displacement due to tsunami load for each variation of tsunami inundation depth. The vulnerability analysis results indicated that retrofitting the school building with concrete jacketing reduces the probability of building damage due to earthquake loads by 18% at the level of complete damage at a PGA of 0.520 g (based on the Indonesian Seismic Map). Similarly, it reduced the probability of building damage due to tsunami loads by 20%, at the level of complete damage corresponding to a tsunami wave height of 5.00 m for West Pasaman, Indonesia.

**KEYWORDS** Shelter School Building; Seismic; Tsunami; Concrete Jacketing; Fragility Curve.

© The Author(s) 2025. This article is distributed under a Creative Commons Attribution-ShareAlike 4.0 International license.

## 1 INTRODUCTION

West Sumatra is a province located in the western part of Indonesia. Geographically, West Sumatra province is a potential source of large-scale earthquakes and tsunamis (Putra et al., 2022). One of the potential sources of this disaster is the movement of the Indo-Australian plate, which moves at 7 mm year<sup>-1</sup> beneath the Eurasian plate. The magnitude of this movement indicates that each plate is actively moving, and this movement causes earthquakes and even tsunamis. In addition, based on historical data, numerous seismic events and occurrences of tsunamis have been documented, arising from the complex interactions of converging plate boundaries within the Sumatra subduction zone (Haridhi et al., 2023), such as the Indo-Australian plate pushing against the stable Indonesian plate. A push beyond the elasticity of the stable plate will generate a major tsunami, such as in 1833 (Mw 9.2), 2005 (Mw 9.3), and most recently 2010 in Mentawai. Recently, more than 61 earthquakes in the area were predicted to be in the megathrust segment with a magnitude of at least 4 Mw (Putra et al., 2022).

The risk of death due to earthquakes and tsunamis is

very high, so good risk management is needed to reduce the number of victims. Disaster management for tsunamis can be improved by mapping evacuation routes and shelters. In several cases, horizontal evacuation does not work, mainly because there is very little road infrastructure in West Sumatra, Indonesia's coastal areas, that is perpendicular to higher ground locations, making it challenging to carry out horizontal evacuation. Consequently, evacuating vertically to multi-story buildings (shelters) around school buildings is necessary when a tsunami warning is given.

Understanding the vulnerability of shelter (escape building) in school areas to tsunamis is critical for developing effective mitigation strategies and increasing the resilience of coastal communities in the education sector. Vulnerability is one reason why, as the schools are not built to be disaster-resilient, countless children's safety is at risk. This dynamic characteristic must be studied by correlating individuals, socio-structural factors, and changing conditions over time (Hansson et al., 2020). In this study, the school building of SDN 02 Sasak Ranah Pasisia in West Pasaman,

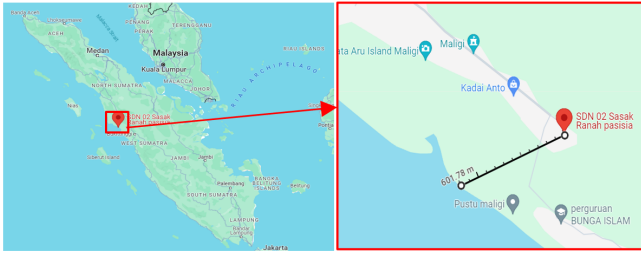


Figure 1 The location of existing shelter school building (Google Maps, 2024).

West Sumatra, Indonesia, is in the category of being vulnerable to earthquakes and tsunamis and requires more attention to the disaster prevention system, so a shelter building is needed in the school area, as shown in Figure 1.

The SDN 02 Sasak Ranah Pasisia, an elementary school, had a shelter building constructed in 2010 (after the 2009 West Sumatra earthquake). However, as of now, the construction remains incomplete (Figure 2a). The shelter building is planned to be a three-story reinforced Concrete (RC) structure with a height of 14.55 m. The building is in the tsunami red zone area, around 0.6 km from the coastal line. Before continuing the construction of this shelter, it is necessary to review the structure's suitability to existing conditions. A visual assessment and concrete testing of the existing building have been carried out. Based on the visual assessment, it was found that cracks appear in the column structure (b), column reinforcement is visible (c), and the concrete cover is peeling off (d), as shown in Figure 2. The method and type of test carried out to evaluate the quality of existing concrete included a hammer test and steel reinforcement using tensile testing of reinforcing bars in the laboratory.

Currently, changes in earthquake regulations and reinforced concrete building construction in Indonesia continue to occur along with the development of engineering science. The design of the school shelter RC building uses old Indonesian building regulations, so it is necessary to evaluate the feasibility of the school shelter building using the current building standards. Apart from regulatory changes, the SDN 02 Sasak Ranah Pasisia school shelter building in West

Pasaman was not planned to withstand tsunami loads by the design consultant, as Indonesia lacks established regulations specifically addressing tsunamis.

In practical terms, the occurrence of a tsunami would inevitably impact the shelter, adversely affecting its strength and capacity to bear the current load potentially resulting in structural damage. A structural assessment using current Indonesian building codes was conducted to proceed with construction and ensure the building's strength against the working loads. In addition, a vulnerability assessment using the fragility curve of this building was developed to observe the probability of structural damage.

Previous studies regarding the vulnerability of school buildings to earthquakes and tsunamis have been undertaken in multiple nations, including Indonesia (Istiqamah et al., 2022), Portugal (Ribeiro et al., 2022), Ecuador (Ballesteros-Salazar et al., 2022), and Japan (Sakurai et al., 2020). However, there is only limited research on the vulnerability of school shelter buildings, which is a solution to school buildings not being tsunami resistant using current regulations. Several factors, such as quality, quantity, and feasibility of continuing the construction of shelter buildings, are considered in determining the aim of this study.

This study evaluates the feasibility of school shelter buildings against earthquake and tsunami hazards using current building regulations before continuing their construction. A solution for retrofitting the building structure was also developed using the concrete jacketing method. Furthermore, the vulnerability of the shelter buildings is evaluated using a fragility curve developed within this investigation, enabling the prediction of potential damage levels in the event of an earthquake and tsunami disaster.

## 2 METHODS

### 2.1 Collecting Shelter School Building Data

This study was conducted in the shelter school building at SDN 02 Sasak Ranah Pasisia, West Pasaman, West Sumatra, Indonesia. This shelter building is an evacuation site for earthquake and tsunami disasters, es-

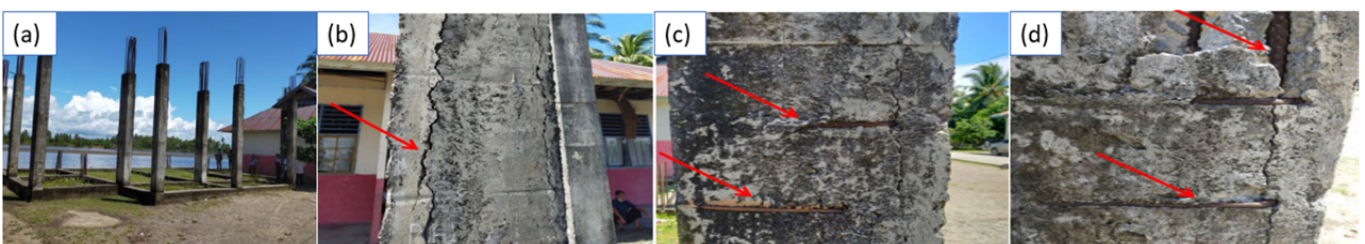


Figure 2 Condition of existing shelter building (a); Crack in the column structure (b); column reinforcement is visible (c); and the concrete cover is peeling off (d)

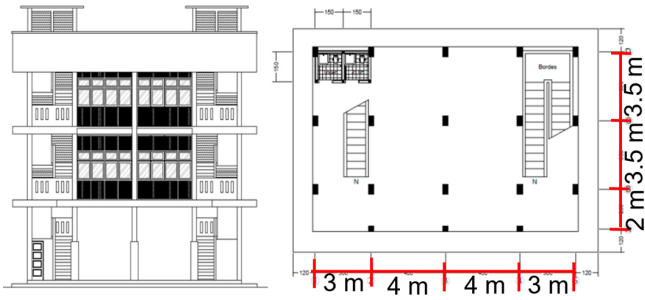


Figure 3 Front view of shelter building (a) and first floor plan (b)

Table 1. Detail of columns

| No. | Type | Disp. Color | Section |     | Flex. Reinf. Bar |         | Shear Reinf. Bar |         |
|-----|------|-------------|---------|-----|------------------|---------|------------------|---------|
|     |      |             | D       | W   | S                | M       | S                | M       |
| 1   | K1   | Red         | 300     | 500 | 16D22            | Ø10-100 | Ø10-200          | Ø10-150 |
| 2   | K2   | Blue        | 300     | 500 | 16D22            | Ø10-100 | Ø10-200          | Ø10-150 |
| 3   | K3   | Brown       | 300     | 500 | 16D22            | Ø10-100 | Ø10-200          | Ø10-150 |
| 4   | K4   | Yellow      | 300     | 300 | 8D19             | Ø10-100 | Ø10-200          | Ø10-150 |

Table 2. Detail of beams

| No. | Type | Disp. Color | Section |     | Flex. Reinf. Bar |      | Shear Reinf. Bar |         |
|-----|------|-------------|---------|-----|------------------|------|------------------|---------|
|     |      |             | D       | W   | T                | C    | T                | C       |
| 1   | B1   | Green       | 450     | 300 | 5D19             | 3D19 | Ø10-100          | Ø10-150 |
| 3   | B2   | Yellow      | 350     | 250 | 4D16             | 2D16 | Ø10-100          | Ø10-150 |
| 4   | B3   | Purple      | 450     | 300 | 4D19             | 2D19 | Ø10-100          | Ø10-150 |
| 6   | B4   | Gray        | 350     | 250 | 3D16             | 2D16 | Ø10-100          | Ø10-150 |

pecially for students who are highly vulnerable when a disaster occurs. It has three floors and is made of Reinforced Concrete (RC).

In this study, the concrete quality, reinforcing steel quality, dimensions of structural elements, and room functions were obtained from as-built drawings (Figure 3). The compressive strength of the existing concrete in the first-floor column is 27.54 MPa, while the planned structural elements for the continued work require a concrete strength of 20.75 MPa, as specified in the plan drawings, and specified density for normal concrete is 2,400 kg m<sup>-3</sup>. The reinforcing steel quality of the longitudinal bar has minimum yield strength,  $f_y = 384$  MPa and minimum tensile strength,  $f_u = 600$  MPa, while the reinforcing steel quality of the ties bar has  $f_y = 235$  MPa and  $f_u = 380$  MPa. The density and elastic modulus of steel bars are 7850 kg m<sup>-3</sup> and 2.105 MPa, respectively. The structure includes main columns and beams with reinforcement bars, detailed in Tables 1 and 2.

In this study, the building is evaluated using tsunami parameters based on the tsunami risk map of West Sumatra and Google Earth with an inundation distance of 2,350 m, building base elevation (z) of 3.4 m, and inundation depth of 5 m from the coastline.

## 2.2 Modeling

Structural modeling is carried out according to the technical data obtained using the finite element software program ETABS v.21. The structural elements, in-

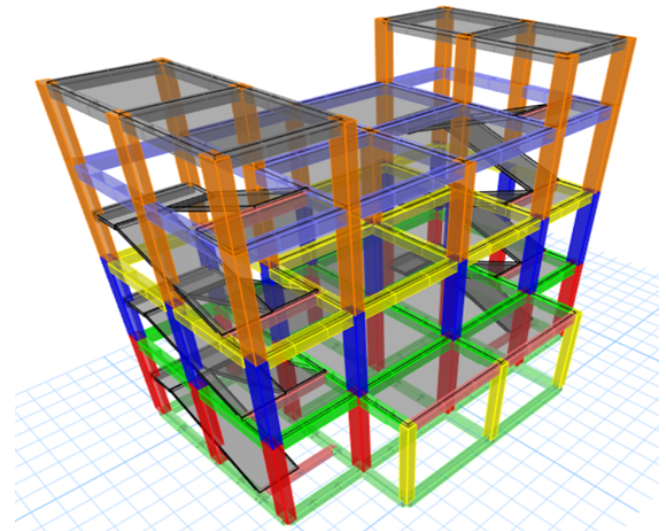


Figure 4 3D Modeling of shelter building

cluding floor slabs, were modeled as thin shells with a rigid diaphragm, and columns and beams, were modeled as frame elements with a fixed support boundary condition. The fixed support boundary condition restricts all translation degrees of freedom for the assigned entities to zero. It is used to model portions of the geometry that are connected to a rigid body. In this study, these rigid bodies are used for ground foundations, column-foundation joints, and beam-column joints. The 3D modeling of the existing building is illustrated in Figure 4.

## 2.3 Loading Analysis

### 2.3.1 Dead Load

According to the Indonesian national standard minimum design load and related criteria for buildings and other structures (Indonesian National Standardization Agency, 2020), the dead load encompasses the total weight of all construction materials installed in a building, comprising walls, floors, roofs, ceilings, stairs, fixed partition walls, finishes, building cladding, and other architectural and structural components, as well as installed service equipment. In this study, the additional dead load on the working floor plate is 1.11 kN m<sup>-2</sup>, and on the concrete deck, the working load is 1.12 kN m<sup>-2</sup>. The weight of the wall above the beam is 8.5 kN m<sup>-1</sup>.

### 2.3.2 Live Load

Based on Indonesian National Standardization Agency (2020), the live load acting on the floor plate has been determined. Live load for the shelter building used the value 4.79 kN m<sup>-2</sup> for concrete slab refuge.



Table 3. Earthquake acceleration data

| Time History Function Name | Direction of the Earthquake | Value (g) |
|----------------------------|-----------------------------|-----------|
| Chichi                     | X                           | 0.580     |
| Chichi                     | Y                           | 0.640     |
| Kobe                       | X                           | 0.610     |
| Kobe                       | Y                           | 0.640     |
| Superstition Hills         | X                           | 0.640     |
| Superstition Hills         | Y                           | 0.636     |

### 2.3.3 Earthquake Load

Earthquake load is an equivalent static load that acts on a building or part of a building to mimics the influence of ground movement due to the earthquake. In this study, the earthquake loads are calculated using parameters based on the Indonesian seismic standard (Indonesian National Standardization Agency, 2019) with shelter building as risk category IV, a priority factor ( $I_e$ ) 1.5, the value of the response modification coefficient ( $R$ ) set at 8, the over-strength factor system ( $\Omega$ ) set at 3, and the deflection magnification factor ( $C_d$ ) set at 5.5, the approach reinforcement parameter ( $C_t$ ) is 0.0466, and the approach period parameter ( $x$ ) is 0.9. The acceleration spectrum parameters are used in the response spectrum design of West Pasaman District, Indonesia.

### 2.3.4 Ground Acceleration Data

The earthquake load will also be analyzed using the time history method so that the acceleration of the earthquake load is compatible with the structure's location. In time history analysis, the selection of earthquake ground motion inputs is crucial for accurately simulating the response of a structure to seismic events. In this study, the selected ground motion records are matched the target response spectrum using ETABS with the response spectrum design of West Pasaman District, Indonesia (location of the existing building). The earthquake acceleration used is shown in Table 3.

The time history analysis considers nonlinear material with parametric strain data, including strain at unconfined compressive strength ( $f'_c$ ) = 0.00192, ultimate unconfined strain capacity = 0.005, and final compression slope (multiplier on E) = -0.1.

### 2.3.5 Tsunami Load

The tsunami loads were calculated based on the Guidelines for Design of Structures for Vertical Evacuation from Tsunamis (FEMA P-646, 2019) with an inundation depth of 5.0 m based on the inundation map of West Pasaman for structural response analysis against the

tsunami loads. In addition, tsunami loads for vulnerability analysis are input at varying tsunami inundation depths of 0.5-5 m with a range of 0.5 m. In this study, the distribution of tsunami loads, such as hydrostatic force, hydrodynamic force, impulse force, and the damming of accumulated waterborne debris, is assigned to structural components such as columns and slabs using the finite element method software ETABS V21 (Fauzan et al., 2023).

FEMA P-646-2019 shows that hydrostatic loads occur when water movement is slow and steady against a structure or structural component. This force always acts perpendicular to the surface of the structural component. A pressure imbalance is caused by differences in water depth on opposite sides of the structure or structural component. Hydrodynamic loads occur when water flows around a structure; hydrodynamic forces are exerted on the structure and individual structural components. These forces are imposed by water flows moving at moderate to high speeds and are a function of the fluid's specific gravity, flow velocity, and geometric structure. Also known as drag forces are a combination of the lateral forces caused by the pressure forces of a moving water mass and the friction forces produced when water flows around a structure or component.

The foremost water waves cause impulse loads that impact the building structure. The value of the impulse load is equal to 1.5 times the hydrodynamic load. The damming of accumulated waterborne debris load, caused by the accumulation of debris carried through water, can be calculated as a hydrodynamic force of increasing magnitude that impedes debris against the front/outer surface of a structure. The tsunami load calculation formula is shown in Table 4.

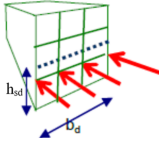
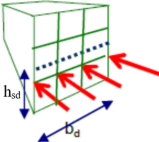
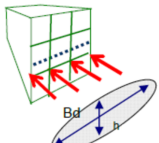
## 2.4 Load Combination

Load combinations, including dead, live, and earthquake loads are calculated based on Indonesian seismic code (Indonesian National Standardization Agency, 2019), while load combinations with tsunami loads are calculated based on FEMA P-646-2019, as shown in Table 5.

## 2.5 Structural Retrofitting

Structural retrofitting is a repair action that increases the strength and stiffness of a building structure. Structural retrofitting is carried out in buildings that have experienced damage due to earthquakes, changes in building function, or the age of the building. It can also be done for existing buildings designed using old regulations that are not strong enough to withstand working loads according to current regulations.

Table 4. Load combination of tsunami forces

| Type of Forces  | Formula   |
|---|---|
| Hydrostatic<br>                                | $Fhs = \frac{1}{2} \times \rho s \times g \times b_d \times h_{sd}^2$ where,<br>Fhs : hydrostatic forces<br>ρs : fluid density including sediment (1100 kg/m <sup>3</sup> )<br>g : gravitational acceleration<br>b <sub>d</sub> : breadth (width) of the wall at the struct. location<br>h <sub>sd</sub> : maximum water height above the base of the wall at the structure location                |
|   | $Fhs = \frac{1}{2} \times C_d \times \rho s \times b_d \times (h_u^2)_{max}$ $(h_u^2)_{max} = gR^2(0.125 \frac{z}{R} + 0.11(\frac{z}{R})^2)$ where,<br>Fd : hydrodynamic forces<br>C <sub>d</sub> : drag coefficient (C <sub>d</sub> = 2.0)<br>h : flow depth<br>u : flow velocity at location of the structure<br>R : design run up elevation<br>Z : ground elevation at the base of the structure |
| Impuls<br>                                   | $Fs = 1.5 \times Fd$ where,<br>Fs : Impuls forces<br>Fd : Hydrodynamic forces   |
| Damming of accumulated waterborne debris<br> | $Fdm = \frac{1}{2} \times C_d \times \rho s \times g \times b_d \times (h_u^2)_{max}$ where,<br>ρs : fluid density including sediment (1100 kg/m <sup>3</sup> )<br>g : gravitational acceleration<br>b <sub>d</sub> : breadth (width) of the wall at the struct. location<br>h : flow depth<br>u : flow velocity at location of the structure   |

Global retrofitting is given to a building structure when it does not meet the structural requirements of the building. In contrast, local retrofitting is given to building structural elements, such as columns and beams, that cannot withstand the working load, such as concrete and steel jacketing.

Numerous methods can be employed for local retrofitting, such as concrete and steel jacketing. The column jacketing method is widely used to enhance the structural capacity of existing columns. This method involves encasing the existing column with a new layer of material, typically concrete or steel, following the installation of additional reinforcement.

Table 5. Load combination

| No | Load combination                 | Note                               |
|----|----------------------------------|------------------------------------|
| 1. | U = 1.4 D                        | Dead load                          |
| 2. | U = 1.2 D + 1.6 L                | Dead and live load                 |
| 3. | U = 1.4 D + L ± 1.3 Ex ± 0.39 Ey | Dead, live, and earthquake loads   |
| 4. | U = 1.4 D + L ± 0.39 Ex ± 1.3 Ey |                                    |
| 5. | U = 0.7 D ± 1.3 Ex ± 0.39 Ey     |                                    |
| 6. | U = 0.7 D ± 0.39 Ex ± 1.3 Ey     | Load combination for tsunamis load |
| 7. | U = 1.2 D + Ts + Lref + 0.25 L   |                                    |
| 8. | U = 0.9 D + Ts                   |                                    |

The process begins with surface preparation, including cleaning and repairing damaged areas. Subsequently, additional reinforcement is installed to augment the strength and stiffness of the column. The new material layer is then applied to form a robust protective layer, usually by pouring or spraying. In this study, local retrofitting using the jacketing method is selected because it effectively enhances the columns' axial, shear, and bending load capacities and improves the structure's earthquake resistance. Furthermore, column jacketing can extend the lifespan of a building by repairing existing damage and increasing the column's load-bearing capacity. Although this process can disrupt building operations and require substantial cost and time, the outcomes are typically beneficial, providing enhanced structural safety and stability.

In this study, the method of retrofitting column structural elements using jacketing involves adding reinforcement and additional dimensions that encase the existing column. Since the jacketing method is applied solely to the column, the reinforced beam-column joint should be designed following seismic design principles by distributing the longitudinal reinforcement of the jacketed column along the beam over a length of 22D. The distribution of additional reinforcement is intended to increase the rigidity of the building, ensuring that when subjected to seismic activity, the structure remains intact and behaves as a cohesive unit. The assessment and retrofitting method flowchart is illustrated in Figure 5.

### 2.6 Development of Fragility Curve

Fragility curve analysis of buildings is an essential tool for evaluating structural vulnerability to seismic events. This analysis involves creating a series of graphs that show the likelihood of a building experiencing different levels of damage during various intensities. The process begins with defining damage states, ranging from minor damage to complete structural failure. Engineers use data from historical earthquakes, simulations, or laboratory tests to establish relationships between ground motion parameters, such as peak ground acceleration (PGA) or spectral acceler-

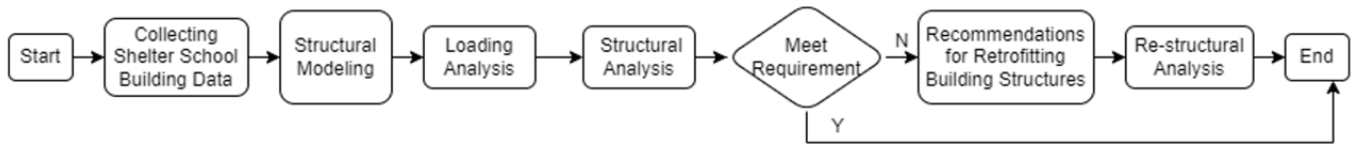


Figure 5 Assessment and retrofitting method flowchart

ation, and the probability of each damage state occurring. These relationships are subsequently plotted as fragility curves.

Fragility curves enable engineers and decision-makers to comprehend the likelihood of different damage scenarios, which is crucial for risk assessment, emergency planning, and mitigation strategies. By identifying the most vulnerable aspects of a building, fragility curve analysis informs the implementation of retrofitting measures and enhances overall seismic resilience. This method provides a probabilistic approach to seismic risk assessment, offering a more nuanced perspective than deterministic methods, and is instrumental in improving the safety and preparedness of communities in earthquake and tsunami-prone areas.

In this study, the probability value of structural damage based on earthquake load and tsunami load levels can be formulated according to the work of (Porter, 2021) through a standard-normal distribution in the following Equation 1 to Equation 4:

$$P = \Phi\left(\frac{\ln\left(\frac{x}{\theta}\right)}{\beta}\right) \tag{1}$$

$$V = \frac{\sigma}{\mu} \tag{2}$$

$$\theta = \frac{\mu}{\sqrt{1 + v^2}} \tag{3}$$

$$\beta = \sqrt{\ln(1 + v^2)} \tag{4}$$

Where  $P$  = Probability of structural damage;  $\Phi$  = the standard normal function;  $x$  = ground motion parameter PGA (g);  $\theta$  = Median demand capacity PGA (g);  $\beta$  = the total uncertainty of the structure;  $v$  = the coefficient of variation of the damage limit;  $\sigma$  = standard deviation of the damage limit;  $\mu$  = mean of the damage limit.

The flowchart of seismic and tsunamis fragility curve development is shown in Figure 6.

### 2.6.1 Seismic fragility curve

A seismic fragility curve is a curve that shows the possibility of damage to a structure when it receives an earthquake load with a certain intensity.

This curve becomes very important in assessing or evaluating the seismic performance of a structure because

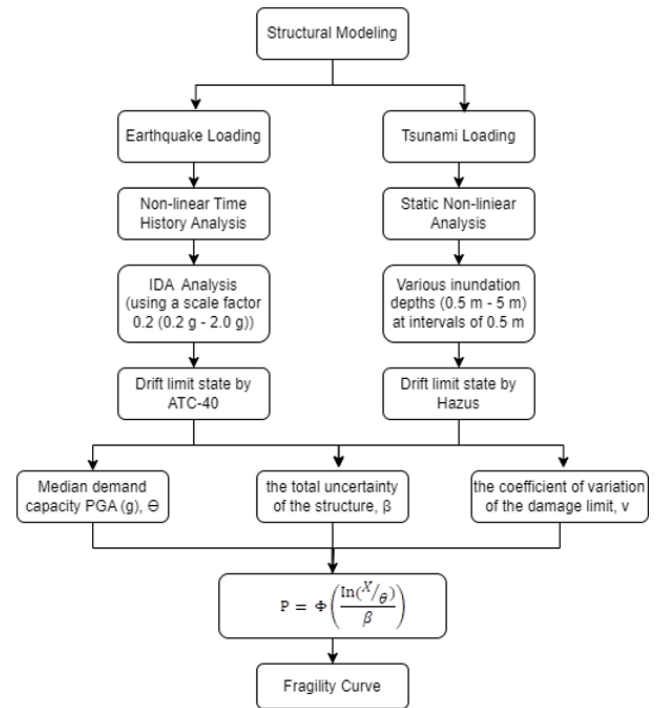


Figure 6 Flowchart of seismic and tsunamis fragility curve development

it displays the level of seismic fragility as possible damage based on earthquake loads that exceed the design load on the performance or limit the state of a particular structure. According to (HAZUS, 2002), the damage state of building structures can be seen in Table 6.

### 2.6.2 Tsunami fragility curve

Tsunami fragility is defined as the probability of structural damage or the fatality ratio, focusing on the hydrodynamic characteristics of tsunami inundation flow, such as inundation depth, current velocity, and hydrodynamic force. The tsunami fragility curve illustrates the relationship between the probability of the extent of structural damage and the tsunami intensity measure ( $IM$ ). The tsunami intensity measure used in this study is tsunami inundation depth (m). In this study, an inundation map of West Pasaman was used to develop a tsunami fragility curve using various inundation depths (0.5 m - 5 m) at intervals of 0.5 m. The damage limit state of buildings due to tsunami loads is depicted in Table 7 (Syamsidik et al., 2020).

Table 6. Damage state due to seismic loads

| Damage State     | Description  |
|------------------|--|
| Slight damage    | Flexural or shear hairline cracks in some beams/columns near or within joints.   |
| Moderate damage  | Most beams/columns exhibit hairline cracks. Some larger cracks indicate that yield capacity has been exceeded.   |
| Extensive damage | Some elements have large flexural cracks and spalling, indicating that ultimate strength has been reached. Some shear failures. Partial collapse may result. |
| Complete damage  | The structure collapses or is in imminent danger of collapse due to brittle failure of non-ductile elements.   |

Table 7. Damage limit state due to tsunami loads

| Damage State     | Description  |
|------------------|--|
| No Damage        | Flooded but no damages found.  |
| Slight Damage    | Damages found windows and doors, no damage on wall and on structural component.            |
| Moderate Damage  | One side wall damages, no damage on column and beam.                                       |
| Extensive Damage | All walls were damaged or roofs felt down, structural components bent/deflected or broken. |
| Complete Damage  | Only floor left.   |

### 3 RESULTS

#### 3.1 Results of Analysis of the Existing Building's Structure

##### 3.1.1 Load-bearing capacity of column

The load-bearing capacity of the columns was analyzed using the P-M column interaction diagram. Based on the results of the P-M interaction diagram, only column K4 (30 × 30) is not capable of withstanding the working load in both the X and Y directions, as P-M values (points) in column K4 (30 × 30) cm have crossed the P-M interaction diagram line, as shown in Figure 7.

The results of the column's shear strength at the support and mid-span are shown in Table 8. The table compares the reduction factor of nominal shear strength ( $\Phi V_n$ ) and ultimate shear force ( $V_u$ ). Only column K4 (30 × 30) has a value of  $V_u$  greater than  $\Phi V_n$ , indicating it is not capable of withstanding the shear strength capacity (Not OK).

##### 3.1.2 Load-bearing capacity of beam

The load-bearing capacity of beam analysis was carried out by reviewing all types of beams on each floor. The results of the beam capacity calculation show that all beams can withstand the moment ( $\Phi M_n \geq M_u$ ) and shear strength ( $\Phi V_n \geq V_u$ ), as shown in Table 9.

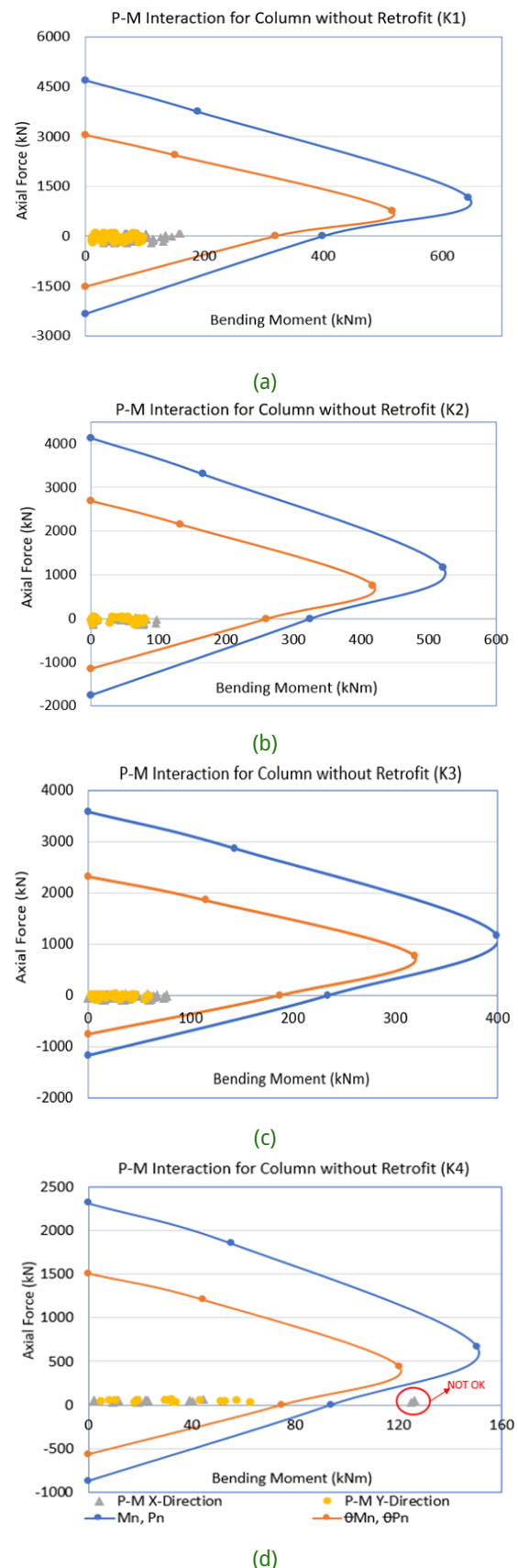


Figure 7 P-M interaction for column without retrofit



Table 8. Shear strength capacity of column

| No. | Type | Section<br><i>D</i> | <i>W</i> | $f_{Vn}$<br>KN | $V_u$<br>KN | $f_{Vn} > V_u$ |
|-----|------|---------------------|----------|----------------|-------------|----------------|
| 1   | K1   | 300                 | 500      | 162.52         | 154.33      | OK             |
| 2   | K2   | 300                 | 500      | 162.52         | 33.61       | OK             |
| 3   | K3   | 300                 | 500      | 162.52         | 50.47       | OK             |
| 4   | K4   | 300                 | 300      | 91.86          | 147.33      | NOT OK         |

Table 9. Moment capacity of beam

| St. | Type Beam | Moment Capacity |              |                   | Shear Capacity |             |                   |
|-----|-----------|-----------------|--------------|-------------------|----------------|-------------|-------------------|
|     |           | $f_{Mn}$<br>kNm | $M_u$<br>kNm | $f_{Mn} \geq M_u$ | $f_{Vn}$<br>kN | $V_u$<br>kN | $f_{Vn} \geq V_u$ |
| 1   | B1        | 178.48          | 97.90        | OK                | 300.34         | 90.07       | OK                |
| 2   | B2        | 178.48          | 73.75        | OK                | 300.34         | 82.07       | OK                |
| 3   | B3        | 178.48          | 48.61        | OK                | 300.34         | 12.07       | OK                |
|     | B4        | 102.96          | 10.49        | OK                | 273.61         | 8.00        | OK                |

### 3.2 Structural Retrofitting Building Using Concrete Jack-eting

Based on the analysis results of the existing building’s structure, several columns, namely column K4 (30 × 30) cm on the 1<sup>st</sup> floor, are unable to withstand the working load. Therefore, it is necessary to perform local retrofitting on the column. Structural retrofitting of the building analysis in this study uses the concrete jacketing method to recover and improve the load-carrying capacity and stiffness of reinforced concrete columns.

In this study, the reinforcement design for column jacketing dimensions and concrete jacketing reinforcement is based on the maximum capacity values ( $P_u$  and  $M_u$ ) from the response results of the existing building structure using the finite element method computer program (ETABS v21).

Figure 8 shows the cross-sectional dimensions and modeling of the retrofitting building structures using concrete jacketing. The building structure was retrofitted by enlarging the cross-sectional dimensions to 50 × 50 cm and adding reinforcement bars to the structural columns to be 12D19. The compressive strength of the additional concrete was 20.75 MPa.

### 3.3 Results of Retrofitted Structural Analysis

#### 3.3.1 Column capacity after retrofitting

Figure 9 shows the P-M interaction diagram of a retrofitted column using jacketing concrete on column K4. It is clear from these figures that all columns have sufficient capacity to withstand the working load, as shown by all P-M values (points) that are within the P-M interaction line. In addition, the shear strength capacity of the column K4-Retrofitted (30 × 50) is able to withstand the P-M interaction, as shown in Table 10.

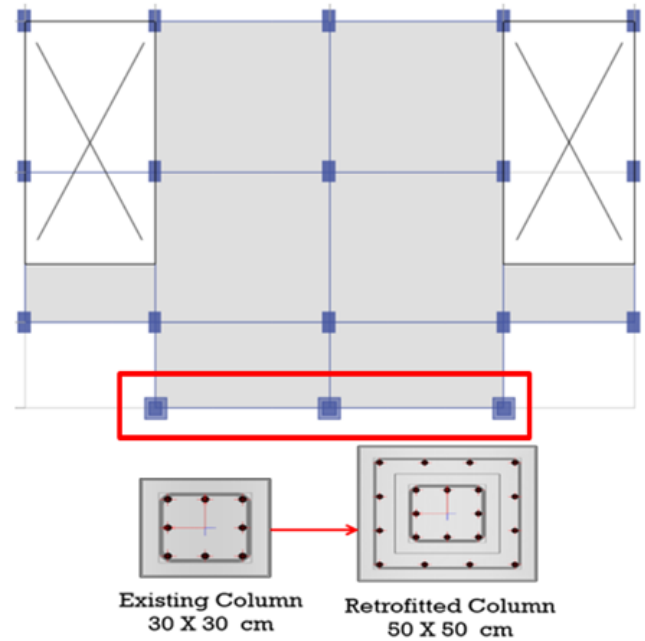


Figure 8 Location of column jacketing and cross-section of retrofitted column

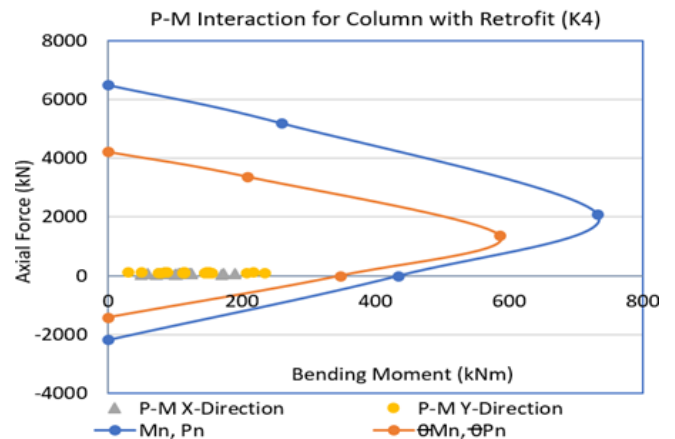


Figure 9 P-M interaction for column K4 with retrofitting

Table 10. Shear strength capacity of columns after retrofitting

| No. | Type    | Section<br><i>D</i> | <i>W</i> | $f_{Vn}$<br>KN | $V_u$<br>KN | $f_{Vn} > V_u$ |
|-----|---------|---------------------|----------|----------------|-------------|----------------|
| 1   | K1      | 300                 | 500      | 162.525        | 125.38      | OK             |
| 2   | K2      | 300                 | 500      | 162.525        | 49.37       | OK             |
| 3   | K3      | 300                 | 500      | 162.525        | 33.64       | OK             |
| 4   | K4-Retr | 500                 | 500      | 217.705        | 157.05      | OK             |

#### 3.3.2 Beam capacity after retrofitting

The beam is a structural component that bears the external load and causes bending moments and shear forces along its span. The results of the calculation of beam capacity after retrofitting show that all beams can withstand the moment ( $\Phi M_n \geq M_u$ ) and shear strength ( $\Phi V_n \geq V_u$ ), as shown in Table 11.



Table 11. Beam capacity after retrofitting

| Type Beam | Moment Capacity |              |                   | Shear Capacity |             |                   |
|-----------|-----------------|--------------|-------------------|----------------|-------------|-------------------|
|           | $f_{Mn}$<br>kNm | $M_u$<br>kNm | $f_{Mn} \geq M_u$ | $f_{Vn}$<br>kN | $V_u$<br>kN | $f_{Vn} \geq V_u$ |
| B1        | 178.48          | 92.97        | OK                | 300.34         | 97.87       | OK                |
| B2        | 178.48          | 73.75        | OK                | 300.34         | 81.13       | OK                |
| B4        | 178.48          | 48.61        | OK                | 300.34         | 53.88       | OK                |
| B5        | 102.96          | 10.50        | OK                | 273.61         | 8.7         | OK                |

### 3.4 Incremental Dynamic Analysis (IDA)

The parameter of the seismic fragility curve requires the maximum displacement of the building, obtained from Incremental Dynamic Analysis and structural modeling responses using the finite element program ETABS. Incremental Dynamic Analysis (IDA) simulates earthquakes of varying intensities applied to the building structure model until collapse occurs.

IDA is utilized here to determine earthquake-induced displacements using a scale factor of 0.2 in the time history method. The acceleration data used in this analysis are from the Chichi Earthquake in Taiwan, the Kobe Earthquake in Japan, and the Superstition Hills Earthquake in the United States. The structural responses regarding displacement due to Incremental Dynamic Analysis are documented for both the X and Y earthquake directions.

### 3.5 Static Non-Linear Analysis due to tsunami forces

The tsunami fragility curve is derived from the maximum displacement due to tsunami loads for each variation of tsunami inundation depth. To develop a tsunami fragility curve using various inundation depths (0.5 m - 5 m) at intervals of 0.5 m.

### 3.6 Seismic Fragility Curve

From these data, adjustments were made to the spectral response of West Pasaman Regency with the soft soil site (SD) class. In this study, the value of limit states follows ATC-40, as shown in Table 12. Subsequently, the seismic fragility curve parameters are plotted using a normal distribution.

Figure 10a and 10b illustrate the result of the seismic fragility curve. Figure 10a shows the seismic fragility curve of the existing building. It can be seen from the figure that the probabilities of slight, moderate, and extensive damage reached 100% and complete damage at 50%. Upon retrofitting with column jacketing, the probability of complete damage decreases to 32% at a PGA of 0.520 g (Figure 10b), according to the Indonesian Seismic Map of the West Pasaman Regency MCER.

Table 12. The limit state by ATC-40

| Damage states | Drift Ratio  |
|---------------|--------------|
| Slight        | 0 - 0.01     |
| Moderate      | 0.01 - 0.02  |
| Extensive     | 0.02 - 0.115 |
| Complete      | 0.115 - 0.33 |

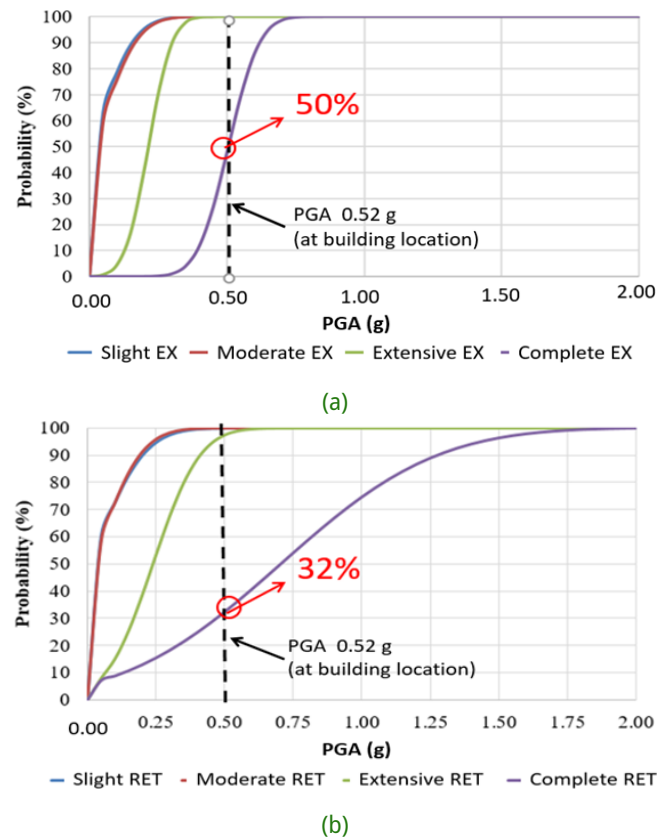


Figure 10 Seismic fragility curve of existing building (a) and the retrofitted building (b)

### 3.7 Tsunami Fragility Curve

Based on the results of maximum displacement due to the tsunami load combination and using Equations (1)-(4), the tsunami fragility curve is determined from the maximum displacement due to the tsunami load for each variation of tsunami inundation depth with damage state limits of tsunami fragility curve by Hazus, as shown in Table 13. Then, the tsunami fragility curve parameters are plotted in a fragility curve using a normal distribution.

The results of the tsunami fragility curve, as illustrated in Figure 11a and 11b, indicate that the existing building has a 90% probability of moderate damage. In contrast, retrofitting with column jackets reduces the probability of moderate damage to 70% for a tsunami inundation depth of 5.00 m in West Pasaman, Indonesia. Other damage levels in existing and retrofitted buildings reached a 100% probability of light damage and a 0% probability of heavy damage and collapse.

Table 13. Damage state limits of tsunami fragility curve

| Damage states | Drift damage index HAZUS (%) |
|---------------|------------------------------|
| Slight        | <0.20                        |
| Moderate      | 0.20 – 0.50                  |
| Extensive     | 0.50 – 1.20                  |
| Complete      | 1.20 – 2.80                  |

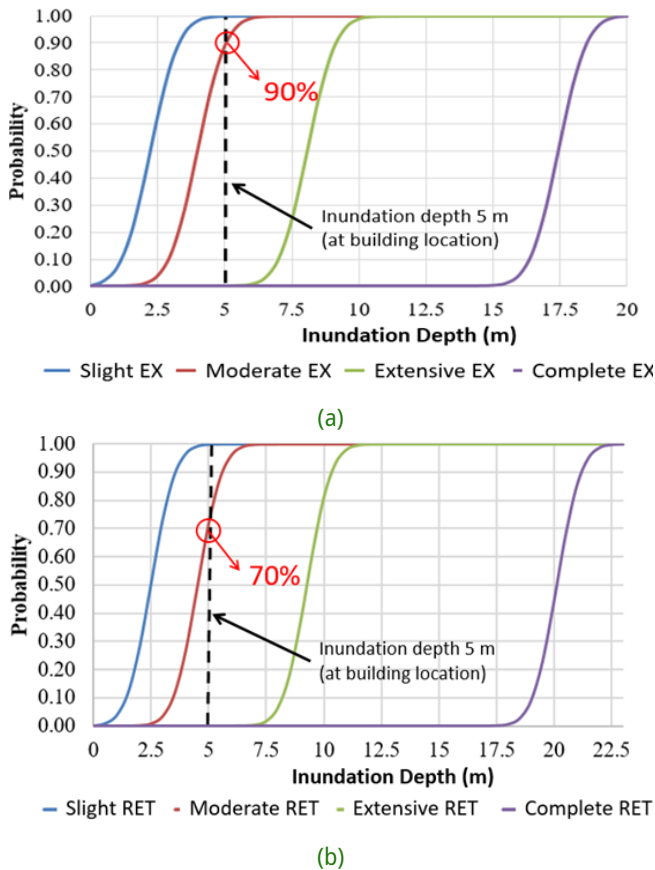


Figure 11 Tsunamis Fragility curve of existing building (a) and the retrofitted building (b)

## 4 DISCUSSIONS

### 4.1 The Effect of Structural Retrofitted Structural Using Concrete Jacketed Columns

Based on the structural analysis of the existing building, it was found that only column K4 (30 × 30 cm) does not meet the current Indonesian building code requirements for withstanding the working load. This is evident in Figure 4, where the P-M values (point) on the interaction diagram exceed the column’s P-M interaction limits. Additionally, the column’s shear capacity is inadequate, with the ultimate shear force ( $V_u$ ) exceeding the reduction factor of the nominal shear strength ( $\Phi V_n$ ). The beam load analysis indicates that all beams can sustain the moment and shear loads acting on the structure, as outlined in Table 9.

Since only a few structural elements are incapable of carrying the load, it is recommended to retrofit them locally, specifically by jacketing the columns.

The re-analysis results using the jacketing retrofit on column K4 demonstrate that all structural elements, including columns and beams, can carry loads in accordance with current standards. The increased dimensions and additional reinforcement of the existing columns significantly enhance the cross-sectional capacity. Assuming that the nominal capacity exceeds the ultimate force acting on the column, the reinforced column exhibits improved strength.

Based on the percentage increase in the capacity of column K4, where the existing dimensions of 30 × 30 cm were strengthened using column jacketing to dimensions of 50 × 50 cm, there was an increase in axial force by 217% (more than two times), bending moment by 386% (almost four times), and shear force by 137%. This significant enhancement in structural performance demonstrates the effectiveness of column jacketing as a retrofitting technique, providing improved load-bearing capacity and resistance to various forces, thereby ensuring greater stability and safety of the structure. Additionally, these improvements suggest the potential for extending the structure’s service life and reducing the need for more extensive and costly repairs in the future.

### 4.2 The Effect of Retrofitting on Seismic Vulnerability of the School Building

Vulnerability analysis of the building structure reveals that retrofitting with concrete jacketing reduces the probability of structural damage due to earthquake loads by 18% at the level of complete damage with a PGA of 0.520 g (based on the West Pasaman Regency MCER Indonesian Seismic Map), as shown in Figures 7a and 7b. According to the seismic fragility curve, this shelter building exhibits a ‘complete’ level of vulnerability under an earthquake with Peak Ground Acceleration (PGA). This vulnerability arises from updated earthquake regulations, which have increased the seismic forces and parameters imposed on structures (Nugroho et al., 2022). Additionally, buildings designed under the old Indonesian seismic code (Indonesian National Standardization Agency, 2019) are highly susceptible to earthquake-induced damage. Therefore, critical buildings must adopt disaster mitigation measures, such as structural strengthening through column jacketing, to ensure they can withstand seismic loads.

### 4.3 The Effect of Retrofitting on Tsunami Vulnerability of the School Building

According to the tsunami fragility curve illustrated in Figures 7c and 7d, the building demonstrates a mod-

erate vulnerability to tsunamis. Structural elements, particularly building columns that initially encounter tsunami waves, are susceptible to experiencing maximum loads. Strengthening these vulnerable structural elements may enhance the building's resilience against tsunamis. Vulnerability analysis of the building structure reveals that retrofitting with concrete jacketing reduces the probability of structural damage due to tsunami loads by 20% at the level of complete damage corresponding to an inundation depth of 5.00 m for West Pasaman, Indonesia. The tsunami fragility curve reveals a significant reduction in moderate damage levels due to the implementation of column jacketing.

## 5 CONCLUSION

The results of this study demonstrate that several columns in the existing building, designed according to the old Indonesian building codes, were unable to withstand working loads, necessitating local retrofitting. The retrofit strategy employs concrete jacketing, involving additional dimensions and reinforcement to restore and enhance the load-carrying capacity and stiffness of reinforced concrete columns. After retrofitting the building column with concrete jacketing, all structural elements demonstrate the capability to withstand earthquake and tsunami loads.

Vulnerability analysis of the building structure reveals that retrofitting with concrete jacketing reduces the probability of structural damage due to earthquake loads by 18% at the level of complete damage with a PGA of 0.520 g (based on West Pasaman Regency MCER Indonesian Seismic Map). Similarly, it decreases the probability of structural damage due to tsunami loads by 20% at the level of complete damage corresponding to an inundation depth of 5.00 m for West Pasaman, Indonesia.

## DISCLAIMER

The authors declare no conflict of interest.

## ACKNOWLEDGMENTS

The authors gratefully acknowledge the financial support provided by Universitas Andalas.

## REFERENCES

Ballesteros-Salazar, K., Caizaguano-Montero, D., Haro-Báez, A. and Toulkeridis, T. (2022), 'Case study of the application of an innovative guide for the seismic vulnerability evaluation of schools located in sangolquí, interandean valley in ecuador', *Buildings* **12**(9), 1471. [URL: https://doi.org/10.3390/buildings12091471](https://doi.org/10.3390/buildings12091471)

Fauzan, Kurniawan, R., Syahdiza, N. and Al Jauhari, Z. (2023), 'Fragility curve of school building in padang city with and without retrofitting due to earthquake and tsunami loads', *International Journal of GEOMATE* **24**(101).

[URL: https://doi.org/10.21660/2023.101.g12251](https://doi.org/10.21660/2023.101.g12251)

Google Maps (2024), 'Google'. [Online] Available at: <https://maps.app.goo.gl/153dSEJ38iYCaeUu5> [Accessed 10 May 2024].

Hansson, S., Orru, K., Siibak, A., Bäck, A., Krüger, M., Gabel, F. and Morsut, C. (2020), 'Communication-related vulnerability to disasters: A heuristic framework', *International Journal of Disaster Risk Reduction* **51**, 101931.

[URL: https://doi.org/10.1016/j.ijdr.2020.101931](https://doi.org/10.1016/j.ijdr.2020.101931)

Haridhi, H., Setiawan, I., Octavina, C., Mahdi, S. and Balqies, C. (2023), 'Tsunami scenario triggered by the activity of the mentawai fault zone offshore western sumatra island', *E3S Web of Conferences* **447**, 01012.

[URL: https://doi.org/10.1051/e3sconf/202344701012](https://doi.org/10.1051/e3sconf/202344701012)

Indonesian National Standardization Agency (2019), *SNI 1726:2019 Seismic Resistance Design Codes for Building and Other Structures*, BSN, Jakarta.

Indonesian National Standardization Agency (2020), *SNI 1727:2020 Minimum Load for Planning of Buildings and Other Structures*, BSN, Jakarta.

Istiqamah, P., Humayra, S. and Huzaim (2022), 'Strengthening capacity study of reinforced concrete school building structure in banda aceh toward earthquakes and tsunami hazards', *E3S Web of Conferences* **340**, 02005.

[URL: https://doi.org/10.1051/e3sconf/202234002005](https://doi.org/10.1051/e3sconf/202234002005)

Nugroho, W., Sagara, A. and Imran, I. (2022), 'The evolution of indonesian seismic and concrete building codes: From the past to the present', *Structures* **41**, 1092–1108.

[URL: https://doi.org/10.1016/j.istruc.2022.05.032](https://doi.org/10.1016/j.istruc.2022.05.032)

Putra, R., Ono, Y., Edidas, Rani, I. and Utama, R. (2022), 'Increasing preparedness against earthquake and tsunami hazards by educating and training a community in sipora island, indonesia', *Aceh International Journal of Science and Technology* **10**(3), 206–217.

[URL: https://doi.org/10.13170/aijst.10.3.23288](https://doi.org/10.13170/aijst.10.3.23288)

Ribeiro, F., Candeias, P., Correia, A., Carvalho, A. and Costa, A. (2022), 'Risk and resilience assessment of lisbon's school buildings based on seismic scenarios', *Applied Sciences* **12**(17), 8570.

[URL: https://doi.org/10.3390/app12178570](https://doi.org/10.3390/app12178570)

Sakurai, A., Sato, T. and Murayama, Y. (2020), 'Impact evaluation of a school-based disaster education program in a city affected by the 2011 great east japan

earthquake and tsunami disaster', *International Journal of Disaster Risk Reduction* **47**, 101632.

**URL:** <https://doi.org/10.1016/j.ijdr.2020.101632>

Syamsidik, Benazir, Luthfi, M., Suppasri, A. and Com-

fort, L. K. (2020), 'The 22 december 2018 mount anak Krakatau volcanogenic tsunami on Sunda Strait coasts, Indonesia: tsunami and damage characteristics', *Natural Hazards and Earth System Sciences* **20**, 549–565.

**URL:** <https://doi.org/10.5194/nhess-20-549-2020>